Available online at www.sciencedirect.com
ScienceDirect
Journal of Sound and Vibration 318 (2008) 715–724
JOURNAL OF SOUND AND VIBRATION
www.elsevier.com/locate/jsvi

Frequency-domain delayless active sound quality control algorithm

Sen M. Kuo[a], Ravi K. Yenduri[a], Abhijit Gupta[b,*]

[a]Department of Electrical Engineering, Acoustics and Vibration Center, Northern Illinois University, DeKalb, IL 60115, USA
[b]Department of Mechanical Engineering, Acoustics and Vibration Center, Northern Illinois University, DeKalb, IL 60115, USA

Received 16 October 2006; received in revised form 5 March 2008; accepted 18 April 2008
Handling Editor: S. Bolton
Available online 13 June 2008

Abstract

This paper presents several broadband active sound quality control algorithms based on delayless frequency-domain techniques and subband adaptive filters. This efficient algorithm provides faster convergence and reduced computational complexity as compared to a time-domain active noise equalizer. An equal-loudness compensation method is also introduced for designing the shaping filter to achieve the desired sound quality. Computer simulations validate this algorithm in applications requiring high-order adaptive filters.
© 2008 Elsevier Ltd. All rights reserved.

1. Introduction

Active noise control is based on the principle of superposition, i.e., an unwanted primary noise is attenuated by a secondary noise of equal amplitude and opposite phase [1,2]. The design of an active noise control system pursues maximum attenuation of the primary noise [3]. However, some applications need to consider psychoacoustics, which concerns the characteristics of the residual noise to match human preference [4]. This demand leads to the extension of active noise control to include acoustic noise shaping for sound quality control. Sound quality is the perceptual reaction to the sound of a product that may affect overall evaluation of that product [5].

Active sound quality control can be realized by a time-domain broadband active noise equalizer introduced in Ref. [6]. This algorithm controls the residual noise spectrum defined by the shaping filter $C(z)$. This filter is designed such that its magnitude spectrum $|C(\omega)|$ determines the desired shape of the residual acoustic noise. The filtered-X least-mean-square algorithm [7] is used to update the coefficients of the adaptive filter $W(z)$ for minimizing a pseudo-error signal instead of minimizing the residual noise in conventional active noise control systems. The time-domain active noise equalizer is optimized to reduce a passband disturbance caused by uncorrelated noise for improved stability [8].

*Corresponding author. Tel.: +1 815 753 9379; fax: +1 815 753 0416.
E-mail address: gupta@ceet.niu.edu (A. Gupta).

0022-460X/$ - see front matter © 2008 Elsevier Ltd. All rights reserved.
doi:10.1016/j.jsv.2008.04.029

Nomenclature

$C(z)$	shaping filter
$d(n)$	primary noise
D	decimation factor
$e(n)$	residual noise
$e'(n)$	pseudo-error
$e'_m(n)$	subband pseudo-error
$E'(k)$	fast Fourier transform of $e'(k)$
$F(z)$	prototype filter
FFT	fast Fourier transform
L	length of the primary adaptive filter
LMS	least-mean-square
m	frequency-bin index
M_1	length of secondary-path estimate filter
P	number of weights for each subband filter
$P(z)$	primary path
$s(n)$	impulse response of the secondary path
$S(z)$	secondary path
$\hat{S}(z)$	estimate of secondary path
$W(z)$	adaptive filter
$x(n)$	reference input
$y(n)$	output of adaptive filter
μ	step size
$\mu_m(n)$	normalized step size
*	linear convolution

In some broadband active sound quality control applications, the length of the adaptive filter can be very long, which results in high computational complexity. This requirement increases the cost of the system and also reduces convergence speed of the LMS algorithm. The computational efficiency resulting from the fast Fourier transform (FFT) has led to the implementation of adaptive LMS algorithms in the frequency domain [9]. Unfortunately, the FFT introduces undesired delay due to block processing of the signal. For active noise control applications, delay critically limits the bandwidth over which noise cancellation can be achieved [2]. In this paper, a delayless frequency-domain broadband active sound quality control system is developed. This system is also modified to further reduce the computational complexity.

In addition, subband methods [10] have also been developed to improve the convergence speed and reduce the computational complexity of high-order adaptive filters. The processing of signals in subbands not only reduces the computational burden because adaptive filtering is performed at a lower decimation rate, but also results in faster convergence because the spectral dynamic range is greatly reduced in each subband. However, similar to frequency-domain adaptive filters, the disadvantage of subband adaptive filters is the introduction of delay into the signal path by the filter bank. To overcome this problem, a delayless subband adaptive filter was developed for active noise control applications [11]. Signal path delay is avoided while retaining the advantages of subband processing. The technique utilized in this paper develops a broadband active sound quality control system based on the delayless subband adaptive filters.

The remainder of the paper is organized as follows. The proposed delayless frequency-domain active sound quality control system is presented in Section 2, and a version using delayless subband adaptive filters is presented in Section 3. Section 4 analyzes the computational complexity of these broadband systems and compares them with the time-domain algorithm introduced in Ref. [6]. The design of shaping filter $C(z)$ with equal-loudness compensation for filter design is presented in Section 5.

2. Delayless frequency-domain active sound quality control systems

The structure of the delayless frequency-domain broadband active sound quality control system is illustrated in Fig. 1 [12]. To avoid the delay caused by collecting N samples before applying a discrete Fourier transform to perform convolution via multiplication in the frequency domain, the adaptive filter $W(z)$, which is a finite impulse response filter, is implemented directly in time domain. However, the filter updating is performed in the frequency domain and the modified spectrum transformed to update the filter coefficients in the time domain. This delayless structure also prevents an undesired circular convolution in frequency-domain filtering. The canceling signal used to drive the secondary source is computed as

$$y'(n) = y(n) - c(n) * y(n) = y(n) - \sum_{m=0}^{N} c(m)y(n-m), \tag{1}$$

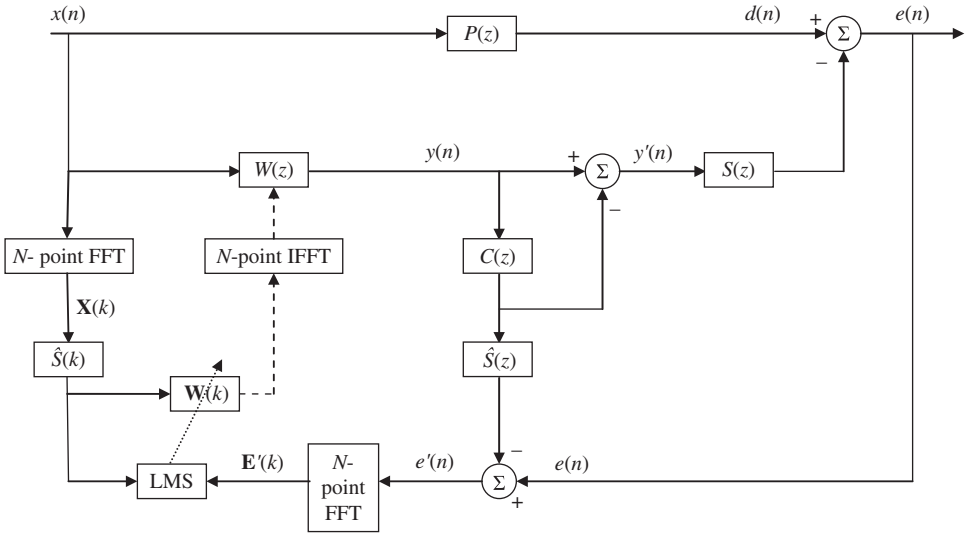

Fig. 1. Block diagram of the delayless frequency-domain active sound quality control system.

where * denotes linear convolution, $c(n)$ is the impulse response of $C(z)$, and $y(n)$ is the output of the adaptive filter $W(z)$. The pseudo-error signal is expressed as

$$e'(n) = e(n) - y(n) * c(n) * \hat{s}(n), \tag{2}$$

where $e(n)$ is the residual noise picked up by an error sensor and $\hat{s}(n)$ is the impulse response of the estimated secondary-path whose transfer function is denoted by $\hat{S}(z)$.

The reference signal $x(n)$ and the pseudo-error signal $e'(n)$ are accumulated in buffers to form N-point blocks $\mathbf{x}(k) = [x(kN-1)\, x(kN-2) \ldots x(kN-N)]^{\mathrm{T}}$ and $\mathbf{e}'(k) = [e'(kN-1)\, e'(kN-2) \ldots e'(kN-N)]^{\mathrm{T}}$, where k is the block index and T denotes the transpose operation. The signal vectors $\mathbf{x}(k)$ and $\mathbf{e}'(k)$ are then transformed once every N samples by an N-point FFT to produce N-point frequency-domain vectors:

$$\mathbf{X}(k) = \mathrm{FFT}[\mathbf{x}(k)] = [X_0(k)\, X_1(k) \ldots X_{N-1}(k)]^{\mathrm{T}} \tag{3}$$

and

$$\mathbf{E}'(k) = \mathrm{FFT}[\mathbf{e}'(k)] = [E'_0(k)\;\; E'_1(k) \ldots E'_{N-1}(k)]^{\mathrm{T}}. \tag{4}$$

The secondary-path estimate $\hat{S}(z)$ and the controller $W(z)$ are represented in the frequency domain as

$$\hat{\mathbf{S}}(k) = [\hat{S}_0(k)\;\; \hat{S}_1(k) \ldots \hat{S}_{N-1}(k)]^{\mathrm{T}} \tag{5}$$

and

$$\mathbf{W}(k) = \mathrm{FFT}[\mathbf{w}(k)] = [W_0(k)\;\; W_1(k) \ldots W_{N-1}(k)]^{\mathrm{T}}. \tag{6}$$

The adaptive filter coefficients are updated in the frequency domain using the complex normalized least-mean-square algorithm [2]:

$$W_m(k+1) = W_m(k) + \mu_m E'_m(k) X'^{*}_m(k), \tag{7}$$

where $m = 0, 1, \ldots, N-1$, is the frequency-bin index, μ_m is the normalized convergence factor based on the corresponding power of the narrowband signal $X'_m(k)$, and

$$X'_m(k) = X_m(k)\hat{S}_m(k), \quad m = 0, 1, \ldots, N-1. \tag{8}$$

The frequency-domain adaptive weight vector $\mathbf{W}(k)$ is updated every N samples. The weight vector $\mathbf{w}(k)$ of the adaptive finite impulse response filter is also updated every N samples using the inverse FFT of $\mathbf{W}(k)$, expressed as

$$\mathbf{w}(k) = \mathrm{IFFT}[\mathbf{W}(k)] = [w(kN-1)\;\; w(kN-2) \ldots w(kN-N)]^{\mathrm{T}}. \tag{9}$$

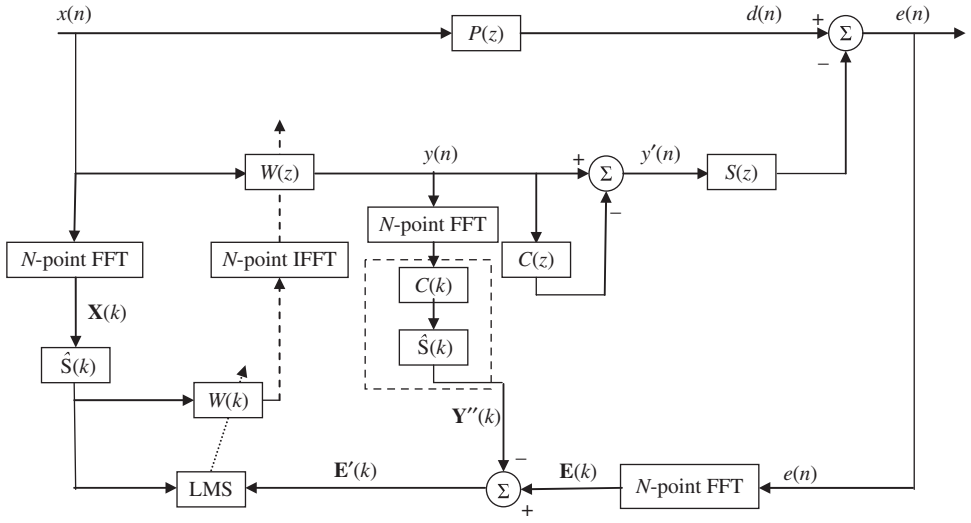

Fig. 2. Modified delayless frequency-domain active sound quality control system.

The output of the adaptive filter is $y(n) = \mathbf{w}^{\mathrm{T}}(k)\mathbf{x}(n)$, where $\mathbf{x}(n) = [x(n)\ \ x(n-1)\ldots x(n-N+1)]^{\mathrm{T}}$ is the signal buffer of $W(z)$ and n is the time index.

The frequency-domain broadband active sound quality control structure shown in Fig. 1 can be further simplified to reduce computation complexity as illustrated in Fig. 2. In this modified frequency-domain delayless active sound quality control system, the pseudo-error vector $\mathbf{E}'(k)$ is obtained once for every N samples. This is accomplished by accumulating the output of the adaptive filter $y(n)$ and the error signal $e(n)$ in buffers to form N-point blocks $\mathbf{y}(k) = [y(kN-1)\ \ y(kN-2)\ldots y(kN-N)]^{\mathrm{T}}$ and $\mathbf{e}(k) = [e(kN-1)\ \ e(kN-2)\ldots e(kN-N)]^{\mathrm{T}}$. The signal vectors $\mathbf{y}(k)$ and $\mathbf{e}(k)$ are then transformed once every N samples by an N-point FFT to produce N-point frequency-domain vectors

$$\mathbf{Y}(k) = [Y_0(k)\ \ Y_1(k)\ldots Y_{N-1}(k)]^{\mathrm{T}} \tag{10}$$

and

$$\mathbf{E}(k) = [E_0(k)\ \ E_1(k)\ldots E_{N-1}(k)]^{\mathrm{T}}. \tag{11}$$

The frequency-domain pseudo-error vector $\mathbf{E}'(k)$ is obtained as $\mathbf{E}'(k) = \mathbf{E}(k) - \mathbf{Y}''(k)$, where $\mathbf{Y}''(k) = [Y_0''(k)\ Y_1''(k)\ldots Y_{N-1}''(k)]^{\mathrm{T}}$ and

$$Y_m''(k) = C_m(k)\hat{S}_m(k)\,Y_m(k), \quad m = 0, 1, \ldots, N-1. \tag{12}$$

If the secondary-path estimate $\hat{S}(z)$ is considered time invariant and obtained using off-line modeling, $\hat{S}_m(k)$ are constants for all k. For a given shaping filter $C(z)$, the product $C_m(k)\hat{S}_m(k)$ can be pre-calculated off-line and used to compute $Y_m''(k)$ during on-line active sound quality control processing.

3. Delayless active sound quality control system using subband adaptive filters

The block diagram of a broadband active sound quality control system using delayless subband adaptive filters [11] is illustrated in Fig. 3. The analysis filterbank typically consists of M bandpass filters. For real signals, only $M/2+1$ of the subband filters $F_0(z)$, $F_1(z)$, …, $F_{M/2}(z)$ are needed. These bands correspond to the positive frequency components of the wideband filter response; the other half is formed by complex-conjugate symmetry. The filtered reference signal $x'(n)$ and the pseudo-error signal $e'(n)$ are decomposed into sets of subband signals using $M/2+1$ single-sideband bandpass filters.

The filtered reference subband signal vector is represented as

$$\mathbf{x}'_m(n) = [x'(nD+m)\ x'((n-1)D+m)\ x'((n-P+1)D+m)]^{\mathrm{T}}, \tag{13}$$

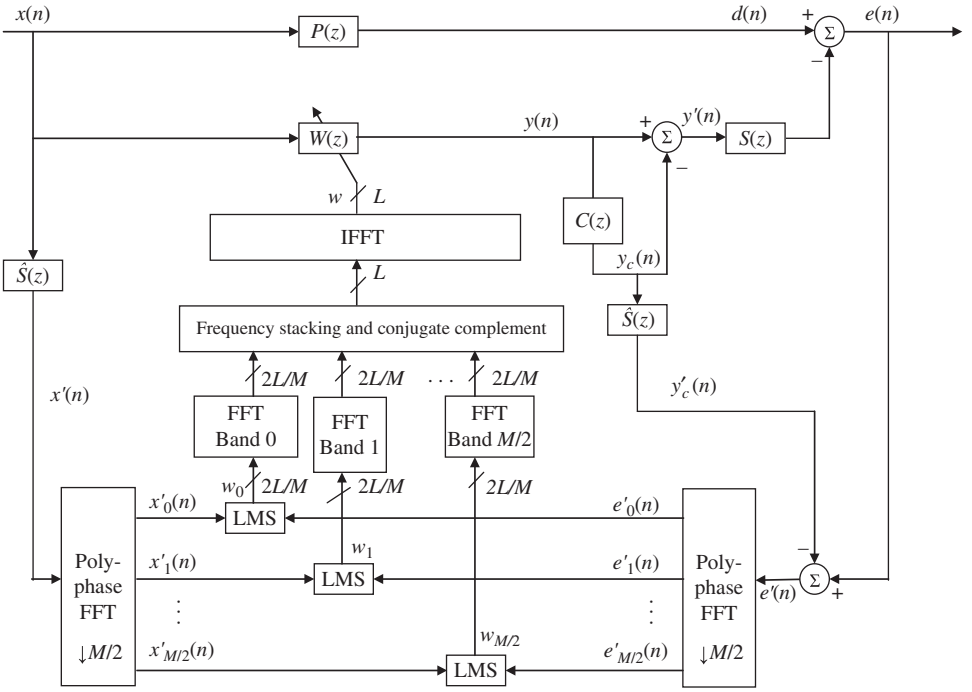

Fig. 3. Delayless active sound quality control system using subband adaptive filters.

where $m = 0, 1, \ldots, D$, the down-sampling factor $D = M/2$, and P is the number of weights for each subband adaptive filter.

The number of subband adaptive filter weights can be determined by the ratio of the number of wideband adaptive filter weights L to the down-sampling factor D, i.e., $P = L/D$. As a result of the decimation factor D, all the subband adaptive filter weights are updated only once for every D samples. The mth subband adaptive filter can be updated using the complex normalized least-mean-square algorithm as

$$\mathbf{w}_m(n+D) = \mathbf{w}_m(n) + \frac{\mu}{\mathbf{x}'^{\mathrm{T}}_m(n)\mathbf{x}'_m(n)}\mathbf{x}'_m(n)e'^{*}_m(n), \tag{14}$$

where $\mathbf{w}_m(n) = [w_{m_0}(n)\ \ w_{m_1}(n) \ldots w_{m_{P-1}}(n)]^{\mathrm{T}}$ is the subband adaptive weight vector for the mth subband. These subband adaptive weights are then transformed to fullband via a weight transformation scheme.

The weight transformation from subband to fullband plays a crucial role in delayless subband adaptive filters. The FFT stacking rules suggested in Ref. [11] are enumerated in Ref. [13] as follows:

1. For $l \in \{0, L/2-1\}$, $W(l) = W_p(q)$, where $W(l)$ and $W_p(q)$ denote the FFT coefficients of the fullband filter and the pth subband filter, respectively; $p = [lM/L]$ where [.], denotes rounding towards the nearest integer; and $q = (l)_{2L/M}$, where $(a)_b$ denotes a modulus b.
2. For $l = L/2$, $W(L/2) = 0$.
3. For $l \in \{L/2+1, L-1\}$, $W(l) = W(L-l)^*$.

The polyphase FFT technique [14] is used to implement the delayless subband adaptive filters. This technique realizes M contiguous single-sideband bandpass filters. Let $F(z)$ denote the prototype filter with K coefficients $[a_0, a_1, \ldots, a_{K-1}]$. The M bandpass filters $F_0(z)$, $F_1(z)$, ... $F_{M-1}(z)$ are obtained as frequency-shifted versions of $F(z)$ such that $F_m(z)$ consists of K coefficients $[a_0,\ a_1\, e^{j2\pi m/K}, \ldots a_{K-1}\, e^{j2\pi m(K-1)/K}]$, where $m = 0, 1, 2, \ldots, M-1$. The output of these subbands are downsampled by a factor $D = M/2$ to produce M complex subband signals. Even numbered subbands are centered at dc, while odd numbered subbands are centered at one half of the decimated sampling frequency [11].

4. Computational complexity

This section evaluates the computational complexity of the different active sound quality control algorithms. The computations required for producing N samples of output is calculated and used for comparison. The following operations are required for all four algorithms:

1. The computation of adaptive filter output

$$y(n) = \sum_{l=0}^{L-1} w_l(n)x(n-l)$$

which requires L multiplications and $L-1$ additions.

2. The computation of shaping filter output

$$y_c(n) = \sum_{k=0}^{K-1} c_k(n)y(n-k),$$

where K is the length of the shaping filter $C(z)$, which requires K multiplications and $K-1$ additions.

The computations required in a time-domain algorithm [6] include the filtered reference signal

$$x'(n) = \sum_{m=0}^{M_1-1} \hat{s}_m x(n-m),$$

where M_1 is the length of the secondary-path estimate filter $\hat{S}(z)$. This requires M_1 multiplications and M_1-1 additions. The output of shaping filter $C(z)$ is fed to $\hat{S}(z)$ to obtain

$$y'_c(n) = \sum_{m=0}^{M_1-1} \hat{s}_m y_c(n-m).$$

This also requires M_1 multiplications and M_1-1 additions. The update equation is

$$w_l(n+1) = w_l(n) + \mu e'(n)x'(n-l), \quad l = 0, 1, \ldots, L-1.$$

This requires $L+1$ multiplications and L additions. Therefore, the total number of multiplications per block is $N(2L+2M_1+K+1)$ and the total number of additions is $N(2L+2M_1+K-2)$.

The different computations required in the frequency-domain active sound quality control algorithm include two N-point FFTs and one N-point inverse FFT as shown in Fig. 1, which require $6N\log_2 N$ multiplications and $6N\log_2 N$ additions. The frequency-domain filtered reference signal

$$X'_m(k) = X_m(k)\hat{S}_m(k)$$

requires N multiplications. The update equation (7) requires $2N$ multiplications and N additions. Therefore, the total number of multiplications required is $N(L+K+M_1)+3N+6N\log_2 N$, and the total number of additions is $N(L+K+M_1-1)+N+6N\log_2 N$.

The computations required in the modified frequency-domain active sound quality control algorithm include three N-point FFTs and one N-point inverse FFT as shown in Fig. 2, which require $8N\log_2 N$ multiplications and $8N\log_2 N$ additions. The frequency-domain filtered reference signal requires N multiplications. The frequency-domain signal $Y''_m(k)$ defined in Eq. (12) requires N multiplications. The frequency-domain pseudo-error signal

$$E'_m(k) = E_m(k) - Y''_m(k)$$

requires N additions. The update equation (7) requires $2N$ multiplications and N additions. Therefore, the total number of multiplications required is $N(L+K)+6N+8N\log_2 N$ and the total number of additions is $N(L+K-1)+3N+8N\log_2 N$.

The different computations required for the broadband active sound quality control algorithm using delayless subband adaptive filters include the filtered reference signal, which requires M_1 multiplications, and M_1-1 additions. The subband filtering for the filtered reference signal and the pseudo-error signal requires

$4P/M + 4\log_2 M$ multiplications and $4(P-1)/M + 4\log_2 M$ additions. The update equation (14) requires $8L/M + 16L/M^2$ multiplications and $8L/M + 16L/M^2$ additions. To transform the subband weights into fullband weights, a $2L/M$-point complex FFT is required for each $M/2+1$ subband. After stacking, an L-point inverse FFT is required to get the fullband weights in the time-domain, all of which requires $2\log_2(2L/M) + (4/M)\log_2(2L/M) + \log_2 L$ real multiplications and an equal number of additions. Therefore, the total multiplications required is

$$N\left(L + K + 2M_1 + \frac{4P}{M} + 4\log_2 M + \frac{8L}{M} + \frac{16L}{M^2} + 2\log_2 \frac{2L}{M} + \frac{4}{M}\log_2 \frac{2L}{M} + \log_2 L\right)$$

and the total additions required is

$$N\left(L + K + 2M_1 - 2 + \frac{4(P-1)}{M} + 4\log_2 M + \frac{8L}{M} + \frac{16L}{M^2} + 2\log_2 \frac{2L}{M} + \frac{4}{M}\log_2 \frac{2L}{M} + \log_2 L\right).$$

Therefore, as the number of subbands M in the polyphase FFT implementation is increased, the computational complexity of the delayless subband broadband active sound quality control system is reduced. The numbers of computations required for generating N samples of output for the time-domain broadband active noise equalizer system, the frequency-domain, and the modified frequency-domain broadband active sound quality control systems are summarized in Table 1. The computational complexity of the algorithms with different numbers of subbands is shown in Table 2. The number of output samples is 25,600.

The delayless subband active sound quality control system has a lower computational complexity than the time-domain algorithm. It is also observed that both frequency-domain broadband active sound quality control systems have a lower computational complexity than the delayless subband active sound quality control system. As the length of the wideband filter and the number of subbands are increased, the difference in the computational requirement for the frequency-domain and the delayless subband broadband active

Table 1
Computational complexities of active sound quality control systems

Type of system	Multiplications for N output samples	Additions for N output samples
Time-domain	$N(2L+2M_1+K+1)$	$N(2L+2M_1+K-2)$
Frequency-domain	$N(L+K+M_1)+3N+6N\log_2 N$	$N(L+K+M_1-1)+N+6N\log_2 N$
Modified frequency-domain	$N(L+K)+4N+8N\log_2 N$	$N(L+K-1)+2N+8N\log_2 N$
Delayless subband	$N\left(L+K+2M_1+\frac{4P}{M}+4\log_2 M + \frac{8L}{M}+\frac{16L}{M^2}+2\log_2\frac{2L}{M}+\frac{4}{M}\times\log_2\frac{2L}{M}+\log_2\frac{2L}{M}+\log_2 L\right)$	$N(L+K+2M_1-2 + \frac{4(P-1)}{M}+4\log_2 M+\frac{8L}{M}+\frac{16L}{M^2} + 2\log_2\frac{2L}{M}+\frac{4}{M}\log_2\frac{2L}{M}+\log_2 L\right).$

Length of wideband filter L, length of shaping filter K, length of secondary path estimate M_1, number of subbands M, and length of prototype filter P.

Table 2
Comparison of computational complexity for multiplications for the systems with different number of subbands

Type of system	Number of subbands			
	8	16	32	64
Time-domain	72,064,000	72,064,000	72,064,000	72,064,000
Delayless frequency-domain	42,163,200	42,163,200	42,163,200	42,163,200
Modified delayless frequency-domain	36,582,400	36,582,400	36,582,400	36,582,400
Delayless subband	82,188,800	63,353,600	55,222,400	51,518,400

sound quality control systems will decrease. Also, as the length of the FFT increases, the difference in the computational requirement between the frequency-domain and the modified frequency-domain broadband active sound quality control systems will decrease.

5. Computer simulation and shaping filter design

Computer simulation is conducted to evaluate the performance of the proposed algorithms. The reference signal is colored noise obtained by passing zero-mean white noise with variance 0.1 through a lowpass filter with a cut-off frequency of 600 Hz. For demonstration purposes, the shaping filter $C(z)$ is a simple bandpass filter with edge frequencies 200 and 400 Hz. The lowpass filter is of the order 128, and the bandpass filter has a length of 204. These filters were designed using the Filter Design and Analysis Tool of MATLAB. The primary-path transfer function $P(z)$ and the secondary-path transfer function $S(z)$ are $P(z) = z^{-6}(1–0.5z^{-1}+z^{-2})$ and $S(z) = z^{-3}$, respectively.

The secondary path was modeled using a 128-tap ($M_1 = 128$) finite impulse response filter $\hat{S}(z)$. For the active sound quality control system using delayless subband adaptive filters, an eight-subband filterbank is used, and each subband has 64 weights. The prototype filter was designed as a lowpass finite impulse response filter with normalized cut-off frequency $\frac{1}{8}(1/M)$. Each filter in the filter bank is a frequency-shifted version of the prototype filter offset by a multiple of π/M. The length of the wideband adaptive filter for all systems is $L = 512$, the FFT length for the frequency-domain active sound quality control systems is $N = 512$, and the length of each subband adaptive filter is $P = 128$.

The magnitude spectra of the residual error signals for the time-domain, delayless frequency-domain, modified delayless frequency-domain, and delayless subband active sound quality control systems are shown in Fig. 4. The sound quality control has the effect of retaining the spectrum represented by the shaping filter $C(z)$ between frequencies 200 and 400 Hz. In this simulation, the last 10,000 samples of the error signal after the convergence of each active sound quality control system is taken as the steady-state signal.

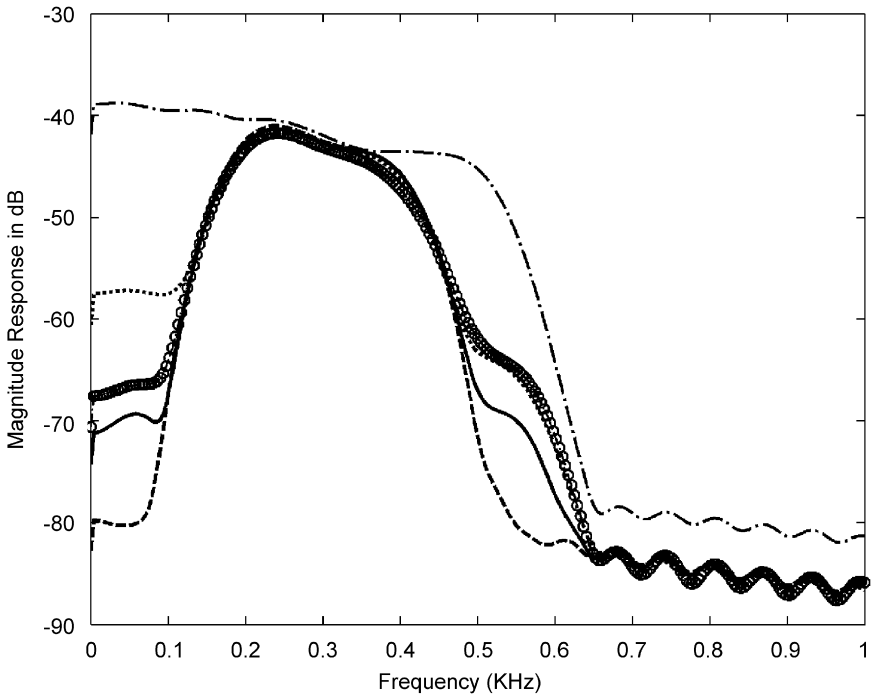

Fig. 4. Comparison of steady-state performance of different active sound quality control systems. – – – Before active sound quality control, - - - - time-domain system, · · · · delayless frequency-domain system, modified delayless frequency-domain system, — delayless subband system.

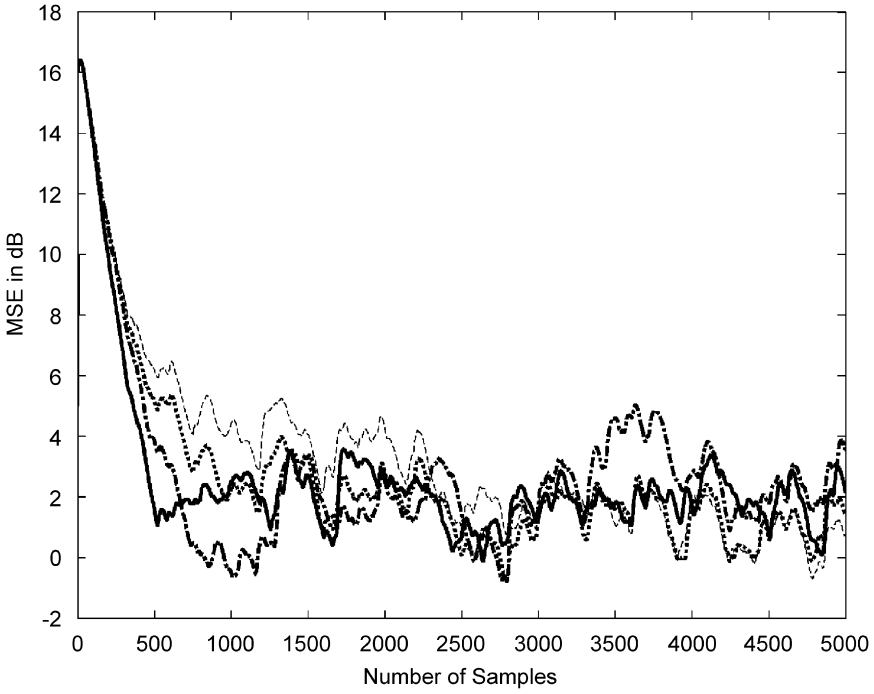

Fig. 5. Comparison of the mean-square error (MSE) convergence among the different active sound quality control systems. – – – time-domain, – - – delayless frequency-domain, · · · · modified delayless frequency domain, —— delayless subband.

The convergence rate is also compared in terms of the mean-square error (MSE) in Fig. 5. The delayless subband active sound quality control algorithm converges faster as compared to the other systems, while the time-domain algorithm has the slowest convergence speed.

According to normal equal-loudness level contours [15], human hearing is not equal for all audible frequencies. The equal-loudness contours show the subjective frequency response of the human ear at various sound pressure levels. In general, noise sounds seem weaker in the bass and treble regions than mid-band when reduced to the same noise level. Examples that use the equal-loudness principle include examining sound quality in the automobile industry, measuring car interior noise, engine noise, exhaust noise, etc. Three curves were created in standards S1.4-1983 [16] and S1.42-2001 [17] for so-called A-weighting, B-weighting, and C-weighting. The s-domain transfer function of the most commonly used A-weighting function is [17]

$$H_A(s) = \frac{4\pi^2 \times 12,200^2 \times s^4}{(s + 2\pi \times 20.6)^2 (s + 2\pi \times 12,200)^2 (s + 2\pi \times 107.7)(s + 2\pi \times 737.9)}. \tag{15}$$

Using the bilinear transform with a sampling frequency of 4 kHz, the z-domain transfer function of the A-weighting filter is approximated as

$$H_A(z) = \frac{0.5835 - 1.167z^{-1} - 0.5835z^{-2} + 2.334z^{-3} - 0.5835z^{-4} - 1.167z^{-5} + 0.5835z^{-6}}{1 - 1.425z^{-1} - 0.97202z^{-2} + 1.8922z^{-3} - 0.0047529z^{-4} - 0.62899z^{-5} + 0.13851z^{-6}}. \tag{16}$$

This function is approximated by a 128-point finite impulse response filter used in the simulations.

For the frequency-domain active sound quality control system with equal-loudness compensation, the shaping filter $C_{el}(z)$ is compensated with the equal-loudness shaping filter as [12]

$$C_{el}(z) = C(z)H_A(z). \tag{17}$$

The residual noise in steady state can be expressed as

$$E(z) = C_{el}(z)D(z) = C(z)H_A(z)D(z), \tag{18}$$

where $D(z)$ is the primary noise. Therefore, the residual noise $e(n)$ not only has the desired shape of the shaping filter $C(z)$, but is also compensated by the equal-loudness function $H_A(z)$.

6. Conclusions

This paper presents the development of delayless frequency-domain algorithms for active sound quality control applications. These algorithms are designed to reduce the computational complexity and increase the convergence rate. Performance of these algorithms is evaluated on the basis of computational complexity, convergence speed, and steady-state residual sound. A broadband active sound quality control system with equal-loudness compensation is proposed to control the residual sound that is equally audible by humans at all frequencies.

References

[1] P.A. Nelson, S.J. Elliott, *Active Control of Sound*, Academic Press, San Diego, 1992.
[2] S.M. Kuo, D.R. Morgan, *Active Noise Control Systems—Algorithms and DSP Implementations*, Wiley, New York, 1996.
[3] P.A. Nelson, A.R.D. Curtis, S.J. Elliott, A.J. Bullmore, The minimum power output of free field point sources and the active control of sound, *Journal of Sound and Vibration* 116 (1987) 397–414.
[4] C. Harris, *Handbook of Acoustical Measurements and Noise Control*, McGraw-Hill, New York, 1991.
[5] R.H. Lyon, *Designing for Product Sound Quality*, Marcel Dekker, New York, 2000.
[6] S.M. Kuo, Y. Yang, Broadband Adaptive Noise Equalizer, *IEEE Signal Processing Letters* 3 (1996) 234–235.
[7] D.R. Morgan, An analysis of multiple correlation cancellation loops with a filter in the auxiliary path, *IEEE Transactions on Acoustics, Speech and Signal Processing ASSP* 28 (1980) 454–467.
[8] S.M. Kuo, A. Gupta, S. Mallu, Development of adaptive algorithm for active sound quality control, *Journal of Sound and Vibration* 229 (2007) 12–21.
[9] J. Ogue, T. Saito, Y. Hoshiko, A fast convergence frequency-domain adaptive filter, *IEEE Transactions on Acoustics, Speech and Signal Processing* 31 (1983) 1312–1314.
[10] J.J. Shynk, Frequency-domain and multirate adaptive filtering, *IEEE Signal Processing Magazine* 9 (1992) 14–37.
[11] D.R. Morgan, J.C. Thi, A delayless subband adaptive filter architecture, *IEEE Transactions on Signal Processing* 43 (1995) 1819–1830.
[12] R.K. Yenduri, Frequency-domain Active Sound Quality Control Algorithms and Applications, M.S. Thesis, Northern Illinois University, 2005.
[13] J. Huo, S. Nordholm, Z. Zang, New weight transform schemes for delayless subband adaptive filtering, *Proceedings of the IEEE Global Communications Conference*, San Antonio, TX, 2001, pp. 197–201.
[14] P.P. Vaidyanathan, Multirate digital filters, filter banks, polyphase network, and application: a tutorial, *Proceedings of the IEEE* 78 (1990) 56–93.
[15] BS ISO, 226: *British Standard Specification for Normal Equal-Loudness-Level Contours for Pure Tones under Free-Field Listening Conditions*, 2003.
[16] ANSI S1.4: *Specifications for Integrating-averaging Sound Level Meters*, 1983.
[17] ANSI S1.42: *American National Standard Design Response of Weighting Networks for Acoustical Measurements*, 2001.